 DOI: 10.1002/masy.200950941

5-Polymer Processing and Composites

Coarsening of PS/SAN Blends with Cocontinuous Morphology Studied with 3D Image Analysis

*Carlos R. Lopez-Barron, Christopher W. Macosko**

Summary: Geometrical parameters of the interface in fluorescently labeled polystyrene (FLPS)/styrene-ran-acrylonitrile compolymer (SAN) blends with cocontinuous morphology were obtained on the basis of differential geometry of 3D images. Images were analyzed for time evolution of interfacial area, average mean and Gaussian curvatures, curvature distributions and topology. Annealing of a symmetric (50/50 FLPS/SAN w/w) and a non symmetric (35/65) blend was monitored. For the symmetric blend a linear time evolution of the characteristic length along with a self similar growth of the microstructure, evidenced by the dynamic scaling of the curvature probability densities, were observed. For the non symmetric blend, the more elongated domains of the minor phase, namely FLPS, broke up producing zones with droplet-matrix structures coexisting with cocontinuous domains. Due to this morphological transition, dynamic scaling failed for the non symmetric blends. The number of holes on the interface, described by the genus, in a fixed sample volume decreases with time due to the growth of the microstructures and the formation of droplets.

Keywords: 3D imaging; blends; cocontinuous; curvature; laser scanning confocal microscopy (LSCM)

Introduction

Due to the highly curved interface between the two phases in cocontinuous blends, an excess free energy is localized at the interface.[1] The necessity to minimize this extra interfacial energy is the driving force for the interfacial evolution (coarsening) towards a less curved surface. Hence the measurement and analysis of the interface curvature is paramount to study the dynamics of coarsening of these blends.

Direct observation and quantification of cocontinuous microstructures have been performed via 2D-imaging with scanning electron microscopy[2,3] or atomic force microscopy.[4,5] However, estimation of 3D geometrical parameters, such as interfacial area per unit volume (Q), from 2D images leads to considerable errors.[3] Additionally, measurements of the surface curvature and topology are not possible from 2D images. Analysis of 3D images allows accurate calculation of geometrical parameters of blend interfaces.[6–9]

Laser scanning confocal microscopy (LSCM) allows one to obtain 3D images of polymer blends[6,9] and after an appropriate analysis to obtain the geometrical parameters of the interface. Jinnai and coworkers used a parallel surface method to measure the area-average mean (H) and Gaussian (K) curvatures of the interface in a poly(styrene-ran-butadiene)/polybutadiene blends[6,8] and a sectioning and fitting method to measure the local values of H and K of a deuterated polybutadiene/

Department of Chemical Engineering and Materials Science, University of Minnesota, Minneapolis, MN 55455-0132
E-mail: macosko@umn.edu

polybutadiene blend.[7,8] Recently we proposed the use of the coordinate transformation (CT) method[10] to compute the local curvature from 3D images of immiscible blends.[9] This method involves the local parametrization of the interface by a quadratic polynomial and the subsequent use of the first and second fundamental forms[11] to compute the local values of H and K.

In the present study we used the CT method to analyze the time evolution of the characteristic length, $\lambda = 1/Q$ (where Q is the interfacial area per unit volume), the curvature distributions and a topological invariant, namely the genus (g), of FLPS/SAN blends with initial cocontinuous morphologies. Two blend compositions were studied: 50/50 and 35/65. Different modes of coarsening were observed for each composition. The microstructure in the symmetric blend grew in a self similar manner, i.e. structures formed at different times are statistically identical while the characteristic length increases. Whereas the non symmetric blend underwent a morphological transition due to the pinch off of the elongated domains of the minor phase (FLPS).

Experimental Part

Materials

FLPS was synthesized via free radical polymerization of styrene (S) with 1% of a fluorescent monomer, namely anthracenylmethyl methacrylate. SAN containing 9.6%mole of acrylonitrile (AN) (measured via CHN analysis) was synthesized from a mixture of S and AN with monomer ratio: S/AN = 4.1. Both polymerizations were performed at 60 °C with AIBN as initiator. The resulting polymers were purified by precipitation in methanol and dried under vacuum for a week. The weight average molecular weight of FLPS and SAN, measured by gel permeation chromatography with polystyrene standards, were 122,000 and 116,000, respectively. The zero shear viscosity, measured with a parallel plate rheometer (ARES, TA Instruments) at 200 °C is 1485 and 2376 Pa-s for FLSP and SAN, respectively.[9]

Blending and Annealing

FLPS/SAN blends with two different compositions, 35/65 and 50/50, were prepared in a 4.3 cm^3 twin screw microcompounder (Daca Instruments) at 180 °C with N2 purge. After 10 min of mixing, the blend was extruded out of the mixer and quenched at room temperature. Small pieces of the extrudate were put in between a glass slide and a cover slip and annealed for different times under N2 at 200 °C.

3D Imaging and Image Analysis

The annealed samples were imaged in a LSCM (Olympus Fluoview 1000) at room temperature with oil immersed 40X and 20X objectives. An incident laser beam of 405 nm and a barrier filter (461 nm), to selectively detect fluorescence from anthracene groups, were used. About 100 2D image slices per sample were taken from 20 to 120 μm away from the cover slip. The 2D images were deconvoluted, thresholded and reconstructed into 3D images using a non structuring method based on the marching cubes algorithm.[12] With this method, a triangular mesh representation of the blend interface is generated.[9]

Differential geometry was applied on the triangular meshes to compute the geometrical parameters of the interface, namely, the specific interfacial area per unit volume (Q) and the local mean (H) and Gaussian (K) curvatures. Q was obtained by simply adding the surface area of all the triangles in the mesh. The local values of H and K were calculated using the CT method.[9,10] This method roughly consists in approximating local surface patches using the quadratic form: $S(u,v) = (u,v,au^2+2buv+cv^2)$. Then, using the definitions of the first and second fundamental forms of differential geometry,[11] we can compute the local curvatures of the corresponding patch as: $H = a+c$ and $K = 4(ac+b^2)$.[9] In this way, the curvature of each triangle in the mesh was calculated and the data from all the triangles

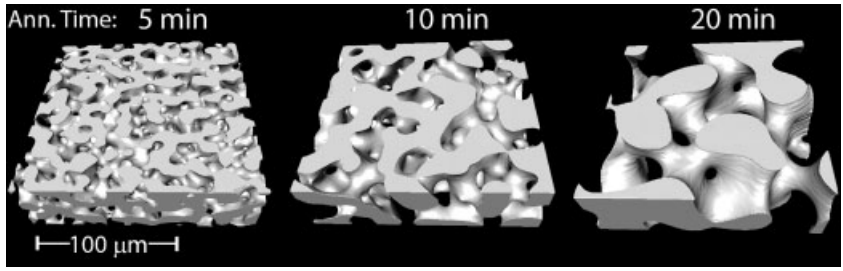

Figure 1.
3D reconstructed images of cocontinuous structures for the 50/50 FLPS/SAN blend at 5, 10 and 20 min of annealing times. The solid part represents the FLPS phase and the transparent part the SAN phase.

(about 10^7 per sample) were used for statistical analysis.

Results and Discussion

Figure 1 shows 3D reconstructed images of the symmetric blend at three different annealing times. From the direct observation of these images, two facts are evident: one is the growth in size of the microstructure with time and second that the cocontinuity remains during annealing. Figure 2 shows the corresponding 3D images of the non symmetric blend. In this case, a transition to a droplet-matrix structure is observed after 20 min of annealing. This process is due to the break up of the more elongated domains formed by the minor phase, i.e. the FLPS.

Figures 3(a)-(b) shows the distribution of the mean and Gaussian curvatures corresponding to the images shown in Figure 1. The probability densities $P_H(H)$ and $P_K(K)$ are defined as:[7,9]

$$P_H(H) = \frac{\sum_{i=1}^{N} A[i|H - \Delta H/2 \le H_i < H + \Delta H/2]}{\Delta H \sum_{i=1}^{N} A_i}, \quad (1)$$

and

$$P_K(K) = \frac{\sum_{i=1}^{N} A[i|K - \Delta K/2 \le K_i < K + \Delta K/2]}{\Delta K \sum_{i=1}^{N} A_i}, \quad (2)$$

where H_i, K_i and A_i are the mean and the Gaussian curvatures and the surface area of the i-th triangle, respectively. ΔH and ΔK are the class intervals of H and K, respectively. The terms in the numerator of equations 1 and 2 accounts for the total surface area of all the triangles that satisfy the conditions: $H\text{-}\Delta H/2 \le H_i < H + \Delta H/2$ and $K\text{-}\Delta K/2 \le K_i < K + \Delta K/2$, respectively. The term in the denominator is included to satisfy the normalization condition:

$$\sum_H P_H(H) \cdot \Delta H = 1 \quad (3)$$

Notice that the $P_H(H)$ distributions are symmetrical and centered in $H = 0$ at each time, evidence that the evolution of the interface progresses along a path of minimal energy. From the P_K distribution, it is evident that the Gaussian curvature is mostly negative at any time, which indicates that the surface is predominantly hyperbolic (i.e. saddle shaped)[11] during the whole coarsening process. In addition, the width of both distributions decreases and its maximum value increases with time, which confirms that the interface evolves towards a more stable state by minimizing its curvature. It is noteworthy that the same characteristics were observed in bicontinuous structures formed from a different mechanism, namely spinodal decomposition.[6–8]

The P_H and P_K distributions for the non symmetric blend are shown in Figures 3(c)-(d). In this case, the P_H distribution is symmetric but not centered in zero at any

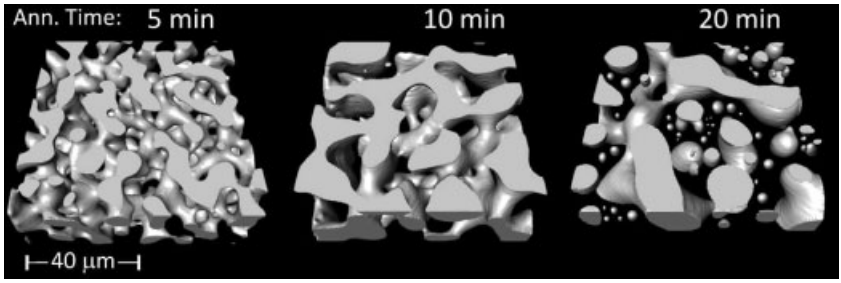

Figure 2.
3D reconstructed images of cocontinuous structures for the 35/65 FLPS/SAN blend at 5, 10 and 20 min of annealing times. The solid part represents the FLPS phase and the transparent part the SAN phase.

time. This result indicates that the interface is globally more curved towards the FLPS phase, which is a consequence of the non-symmetric volume ratio. This effect is more pronounced (i.e. H is globally more positive) at later times due to the formation of droplets which have positive H. The initial P_K distribution, similar to the symmetric case, is predominantly populated in the $K<0$ region. However, due to the growing population of spherical droplets, after the onset of pinch-off, the P_K distribution shifts towards positive values of K.

The time evolution of the characteristic length ($\lambda \sim 1/Q$) of the blends is shown in Figure 4. A linear growth is observed for

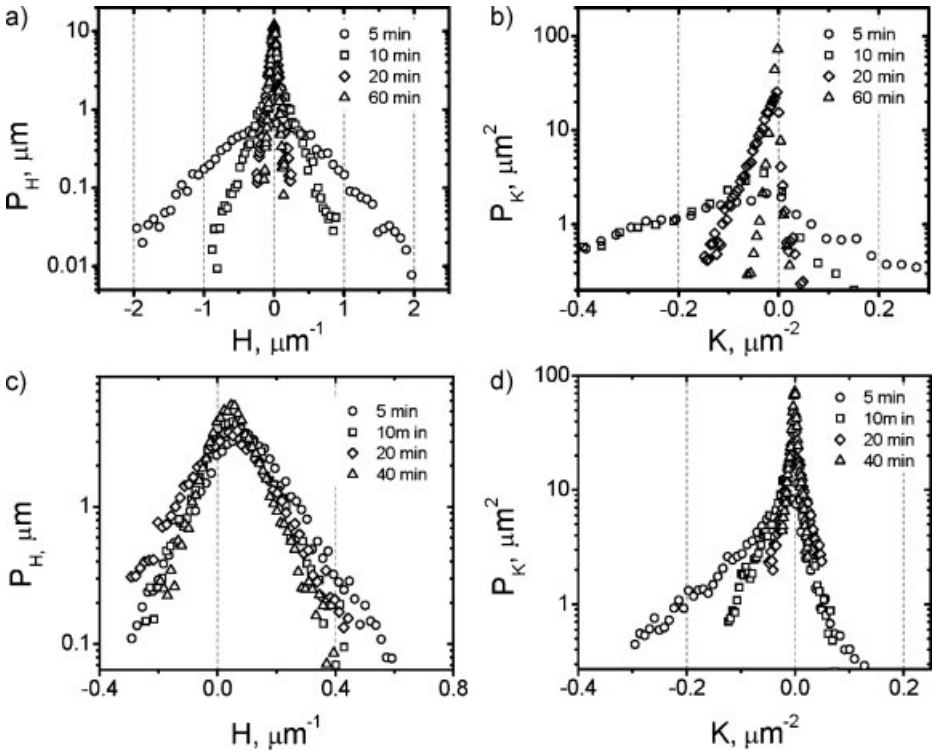

Figure 3.
Probability densities of the mean ((a) and (c)) and the Gaussian ((b) and (d)) curvatures of the interface for the 50/50 ((a) and (b)) and 35/65 ((c) and (d)) FLPS/SAN blends, at different annealing times.[9]

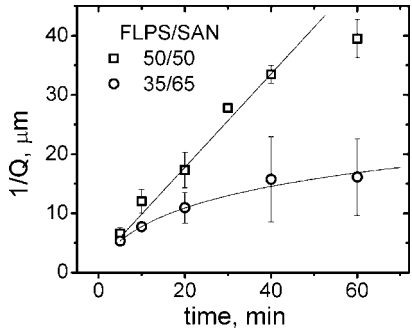

Figure 4.
Inverse of interfacial area per unit volume (1/Q) vs annealing time of FLPS/SAN blends measured from LSCM images. Lines are to guide the eye and the error bars indicate the standard deviation calculated from measurements of five different samples.

the symmetric blend up to 40 min of annealing as described by Siggia,[13] who, considering a capillary flow driven by interfacial tension, obtained the relation: $\lambda = \Gamma/\eta \cdot t$, where Γ is the interfacial tension and η is the blend viscosity. This result assumes that connectivity is maintained towards the coarsening process. After 40 min, a slowing down of the coarsening was observed. This phenomenon is due to a decrease in the global interface curvature which reduces the coarsening driving force, i.e. the interfacial energy. For the non symmetric blend, the increase of λ is not linear. The growth of λ slows down with time due to the formation of droplets which are kinetically more stable than the interconnected domains. Figure 5 show the normalized probabilities densities for the symmetric blend. P_H was normalized with $1/Q$ and P_K with $1/Q^2$. All the normalized curves superimpose with each other, which indicates that the local shape of the interface evolves with self-similarity until an annealing time of 60 min. This behavior was also observed by Nishikawa et al. in partially miscible blends undergoing spinodal decomposition.[7]

The topology of surfaces is related to the area integral of the Gaussian curvature (also called the integral curvature) via the Gauss-Bonnet theorem:[11]

$$\iint_{Surf} K da = 2\pi\chi = 4\pi(1-g), \tag{3}$$

were χ and g are the Euler-Poincaré characteristic and the genus, respectively. These quantities are topological invariants of the surface, i.e. they do not depend on the shape of the surface. The genus, for instance, gives the number of holes in the surface, provided that the surface is closed. For an infinitely interconnected structure, g is infinite; while for a sphere $g = 0$. The data of surface area and local Gaussian curvature in all the triangles in the mesh were used to numerically calculate the integral curvature and the genus using equation 3. Figure 6(a) shows the genus per unit volume, g/V, for the 35/65 and 50/50 blends. For both compositions g/V decreases with time, indicating that for a fixed volume, the number of holes in the interface decreases

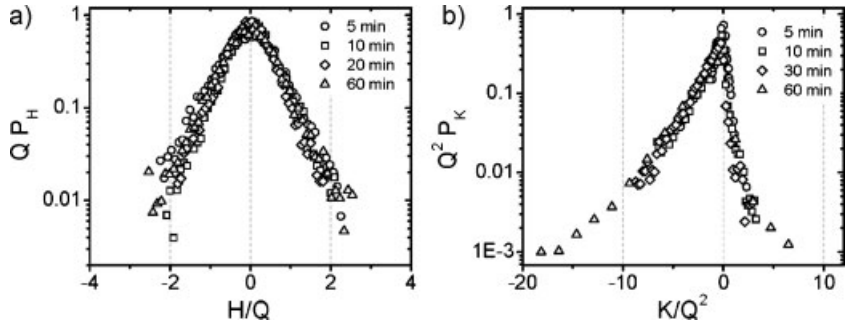

Figure 5.
Scaled probability densities of (a) the mean and (b) the Gaussian curvatures of the 50/50 FLPS/SAN blend interface at different times of annealing.[9]

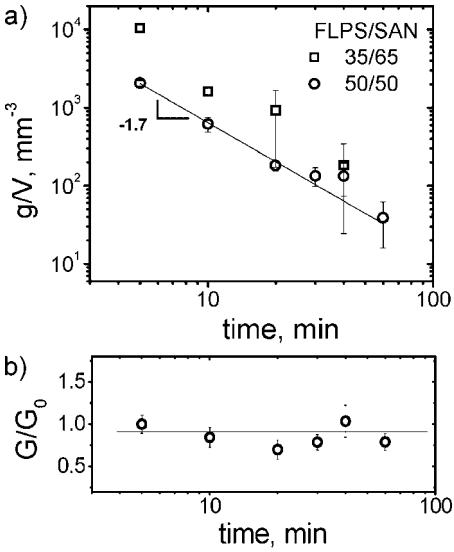

Figure 6.
(a) Genus per unit volume for the FLPS/SAN blend[9] and (b) scaled genus, G, normalized with Go = G(t = 5min) for the FLPS/SAN blend as a function of annealing time. Error bars represent the standard deviation calculated from measurements of 5 different samples.

as the coarsening proceeds. In the symmetric blend this can be confirmed by observing the micrographs in Figure 1 where equal volumes of the symmetric blend with different coarsening times are shown. It is evident that the number of holes (the interconnecting channels) decreases due to the increase of the hole sizes. For the case of the non symmetric blends, the decrease of g/V was due to two factors: the growth in size of the interconnecting channels, and the formation of droplets.

Considering, for the symmetric blend, the evolution laws of the characteristic length, i.e. $\lambda \sim 1/Q \sim t$ and of the genus, i.e. $g/V \sim t^{-1.7}$, we defined a "scaled" genus as: $G = g/(V \cdot Q^{1.7})$, which is independent of the sample size.[9] Note, in Figure 6(b), that this parameter is quite constant throughout the coarsening process, indicating that G scales dynamically with the characteristic length, the same as the curvature distributions. This finding is another indication that the microstructure of this blend grows in a self-similar manner.

Conclusion

The CT method was used to measure the local curvature of the interface of immiscible blends made of FLPS/SAN with two different compositions: 50/50 and 35/65. Probability densities of the mean and Gaussian curvature were obtained and analyzed at different annealing times. For the symmetric blend, a linear growth of the characteristic length along with a self similar evolution of the interface shape were observed. Due to a morphological transition (droplet formation), the growth of the non symmetric blend was neither linear nor self similar. The genus was computed from the data of local values of K using the Gauss-Bonnet theorem. The evolution of the genus per unit volume, g/V, evidences a decrease of the number of holes with time for both compositions, which is due to the increase in size of the characteristic length. For the case of non symmetric blends the decrease of g/V is also due to the formation of droplets.

[1] P. de Gennes, F. Brochard-Wyart, D. Quere, "*Capillarity and wetting phenomena: Drops, bubbles, pearls, waves*", Springer, New York **2004**.
[2] Z. Yuan, B. D. Favis, *AIChE J.* **2005**, *51*, 271.
[3] A. Pyun, J. R. Bell, K. H. Won, B. M. Weon, S. K. Seol, J. H. Je, C. W. Macosko, *Macromolecules* **2007**, *40*, 2029.
[4] M. Lavorgna, G. Mensitieri, G. Scherillo, M. T. Shaw, S. Swier, R. A. Weiss, *J. Polym. Sci. B: Polym. Phys.* **2007**, *45*, 395.
[5] J. Zhang, S. Ravati, N. Virgilio, B. D. Favis, *Macromolecules* **2007**, *40*, 8817.
[6] Y. Nishikawa, H. Jinnai, T. Koga, T. Hashimoto, S. T. Hyde, *Langmuir* **1998**, *14*, 1242.
[7] Y. Nishikawa, T. Koga, T. Hashimoto, H. Jinnai, *Langmuir* **2001**, *17*, 3254.
[8] H. Jinnai, Y. Nishikawa, T. Ikehara, T. Nishi, *Adv. Polym. Sci.* **2004**, *170*, 115.
[9] C. R. Lopez-Barron, C. W. Macosko, *Langmuir*, Accepted (to be published in August 18, 2009).
[10] P. T. Sander, S. W. Zucker, *Proc. 1rst Int. Conf. Comput. Vision* (London) **1987**, 231.
[11] A. Gray, E. Abbena, S. Salamon, "*Modern Differential Geometry of Curves and Surfaces with Mathematica*", 3rd ed., Chapman & Hall/CRC, Boca Raton 2006.
[12] W. E. Lorensen, H. E. Cline, *Comput. Graph.* **1987**, *21*, 163.
[13] E. D. Siggia, *Phys. Rev. A* **1979**, *20*, 595.

